Available online at www.sciencedirect.com
ScienceDirect
Bioelectrochemistry 72 (2008) 66–76
Bioelectrochemistry
www.elsevier.com/locate/bioelechem

Kinetic studies of glucose oxidase in polyelectrolyte multilayer films by means of scanning electrochemical microscopy (SECM)

Malte Burchardt, Gunther Wittstock *

Carl von Ossietzky University of Oldenburg, Faculty of Mathematics and Science, Center of Interface Science (CIS), Department of Pure and Applied Chemistry and Institute for Chemistry and Biology of the Marine Environment, D-26111 Oldenburg, Germany

Received 31 July 2007; received in revised form 26 October 2007; accepted 10 November 2007
Available online 3 January 2008

Abstract

Multilayer films of glucose oxidase (GOx) and poly(dimethyl diallyl ammonium chloride) (PDDA) prepared by layer-by-layer deposition were studied using scanning electrochemical microscopy (SECM). Aminated glass slides were coated with five bilayers of poly(styrene sulfonate) (PSS) and PDDA and used as substrates onto which GOx/PDDA multilayers were deposited. UV–Vis experiments confirmed multilayer growth, scanning force microscopic images provided morphological information about the films. SECM current–distance curves enabled the determination of kinetic information about GOx in GOx/PDDA multilayers as a function of layer number, film termination, inert covering layers, and enzyme substrate concentration after fitting to numerical models. The results indicate that only the topmost layers contributed significantly to the conversion. An odd–even pattern was observed for PDDA-terminated films or GOx-terminated films that correlated with morphological changes.

Keywords: Scanning electrochemical microscopy (SECM); Layer-by-layer deposition; Glucose oxidase; Scanning force microscopy; Polyelectrolytes

1. Introduction

Popularised in the 1990s by Decher and Hong [1,2], layer-by-layer (LbL) deposition of polyelectrolytes (PE) on charged surfaces found widespread application in thin film preparation. Biological molecules can be incorporated in LbL films if the pH during deposition differs from their isoelectric point. This approach has been used to obtain functional films [3–5]. Probably due to mild adsorption conditions and preferable microenvironments in the films, many enzymes kept their activity after immobilisation [6]. Numerous studies investigated the growth of enzyme/PE multilayer films and the activity of incorporated enzymes. Most often, spectrophotometrical and electrochemical methods were employed to measure enzymatic reaction [7–12]. For electrochemical experiments, multilayer films were deposited onto electrode surfaces and mediated electron transfer between redox-enzymes and the supporting electrode surface, or the detection of reaction products at the supporting electrode were used to monitor the enzyme reaction rate [9–15]. The mediator may be provided in bulk solution or co-immobilised in the film. LbL deposition of enzyme layers represents an attractive non-manual way of enzyme immobilisation both on conducting surfaces (e.g. for amperometric sensors) as well as on insulating surfaces (e.g. for microreactors or optical sensors) [16]. The substrates can be templated by charged monolayers providing access to micropatterened PE films [17].

Scanning electrochemical microscopy (SECM) is a scanning probe technique that uses a positionable ultramicroelectrode (UME) as probe [18–20]. It is a powerful tool that enables mapping local chemical reactivities at interfaces and extraction of local kinetic data of heterogeneous reactions. The latter are obtained by recording current–distance curves in the so-called feedback mode where a mediator provided in the bulk solution is converted at the UME and its recovery at the sample surface is determined and compared to numerical simulations [21–23]. A large number of systems has been investigated including pioneering work on glassy carbon electrodes [22], semiconduc-

* Corresponding author. Tel.: +49 441 798 3971; fax: +49 441 798 3979.
E-mail address: gunther.wittstock@uni-oldenburg.de (G. Wittstock).

1567-5394/$ - see front matter © 2007 Elsevier B.V. All rights reserved.
doi:10.1016/j.bioelechem.2007.11.010

tors [24], enzyme layers [25] and so forth. SECM-based determination allows kinetic investigations of enzymes immobilised on microstructured insulating supports such as glass, polymeric membranes, microbeads etc. [26–31].

Our long term goal is the preparation and characterisation of patterned enzymatically active microstructures based on LbL films. In this study, PE multilayer films consisting of GOx and PDDA were prepared on an insulating support. UV–Vis measurements confirmed multilayer growth, AFM images provided morphological information. Using SECM approach curves, local kinetic information of the embedded enzyme was obtained. Their kinetics were characterised with respect to layer number, film termination, substrate concentration, and inert PE termination layers in order to analyse the interplay between diffusion in the solution, mass transport in the film and local enzymatic activity.

2. Materials and methods

2.1. Materials

The following chemicals were used without further purification: polystyrene sulfonate (PSS, MW ~70,000 g mol^{-1}, 30% in water, Aldrich, St. Louis, MO, USA), poly(diallyl dimethyl ammonium chloride) (PDDA, MW 100,000–200,000 g mol^{-1}, 20% in water, Aldrich, St. Louis, MO, USA), glucose oxidase (GOx, from *Aspergillus niger*, EC 1.1.3.4, 40,300 units g^{-1}, Sigma, St. Louis, MO, USA), NaCl (Sigma, St. Louis, MO, USA), ferrocene methanol, (Fc, ABCR GmbH, Karlsruhe, Germany), $Na_2HPO_4{\cdot}2H_2O$ (Scharlau, Barcelona, Spain), $NaH_2PO_4{\cdot}2H_2O$ (Fluka, Buchs, Switzerland), and D-(+)-glucose (99.5%, Sigma, St. Louis, MO, USA). Solutions were prepared using deionised water obtained from a water purification system (resistance >18.2 Ω cm^{-1}, Seralpur PRO 90 C, Seralpur, Ransbach, Germany). Aminated microscope slides of glass were obtained from Menzel-Glaeser (Braunschweig, Germany).

2.2. Sample preparation

A precursor layer consisting of five bilayers of PSS and PDDA [$(PSS/PDDA)_5$] was deposited on aminated glass slides by alternating dipping of the substrate in 1 mg mL^{-1} polyelectrolyte solutions (in 0.1 mol L^{-1} NaCl, pH 4.5±0.1, adjusted using 5 mmol L^{-1} HCl) and intermediate excessive rinsing with deionised water. $(GOx/PDDA)_n$ multilayers as well as the $(PSS/PDDA)_m$ covering layers were prepared by alternating adsorption from 1 mg mL^{-1} solutions without salt. Dipping solutions and water for rinsing were adjusted to pH 7 using 5 mmol L^{-1} NaOH. GOx is negatively charged at this pH (isoelectric point 4.2 [32]) and can be deposited as a polyanion with an appropriate polycation (e.g. PDDA) by the LbL technique.

2.3. UV–Vis spectroscopy

Transmission spectra of PE multilayer films were obtained using a fiber-optic CCD spectrometer (getspec-2048UV/NIR, 25 μm entry slit, Sentronic, Dortmund, Germany) with a deuterium–halogen light source (getLight-DHS, Sentronic). A spectrum was collected after deposition of each double layer and drying with compressed air. The reference spectrum was obtained from aminated glass coated with the $(PSS/PDDA)_5$ precursor layer.

2.4. Scanning electrochemical microscopy

The SECM approach curves were recorded on two home-built instruments described elsewhere [33–35]. UME were obtained by sealing Pt wires (25 μm diameter, Goodfellow GmbH, Bad Nauheim, Germany) into borosilicate glass capillaries (Hilgenberg GmbH, Malsfeld, Gemany) and shaping the apex according to Ref. [36]. The electrodes had a ratio $RG \approx 10$ between the radius r_{glass} of the insulation sheath and the radius of the active electrode area r_T. A Pt wire as auxiliary electrode and a Ag|AgCl|3 M KCl reference electrode, to which all potentials are referred, completed the electrochemical cell. The SECM operated either with the monopotentiostat μ-P3 (Schramm, Heinrich Heine University, Düsseldorf, Germany) or the biopotentiostat CHI 7001B (CH Instruments, Austin, TX, USA). The substrate solution contained 0.045–0.9 mmol L^{-1} Fc and 10–100 mmol L^{-1} glucose in 0.1 mol L^{-1} phosphate buffer (pH 7.0) and 0.1 mol L^{-1} NaCl. Before the experiment, the solution was bubbled with inert gas (N_2 or Ar) for several minutes and a gentle stream of inert gas was passed over the electrochemical cell during the measurement. The potential of the UME was held at $E_T = +300$ mV and moved at $v_T = 0.87$ μm s^{-1}.

2.5. Scanning force microscopy

AFM micrographs were recorded in Tapping Mode™ with a RTESP probe using a Nanoscope IIIA controller and a Dimension 3100 sample stage (Veeco Instruments Inc., Santa Barbara, CA, USA). Root mean square (RMS) values as indication of surface roughness were determined on an area of 1 μm^2 using the Nanoscope software, version 5.30r3sr3.

3. Results and discussions

3.1. Multilayer growth

Fig. 1A shows transmission UV–Vis difference spectrum of GOx–PDDA multilayers with 7 double layers on top of 5 double layers PSS–PDDA $[(PSS/PDDA)_5–(GOx/PDDA)_7]$ vs. the precursor layer $(PSS/PDDA)_5$ on an aminated glass slide. The signal is rather weak and therefore the spectrum is noisy. The absorption peak at appr. 670 nm can be ascribed to GOx. It does not appear in the spectra of the corresponding $(PSS/PDDA)_n$ multilayer. The peak area has been determined between 640 nm and 705 nm for $(GOx/PDDA)_n$ with $1 \le n \le 9$. After the second double layer the absorption peak area increases linearly confirming the regular growth of multilayer films (Fig. 1B).

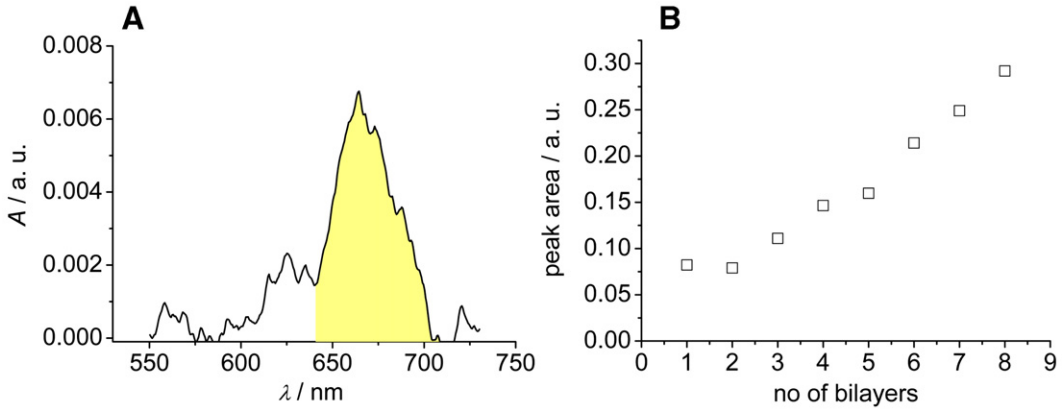

Fig. 1. UV–Vis difference spectra of $(PSS/PDDA)_5$–$(GOx/PDDA)_n$ vs. $(PSS/PDDA)_5$ on aminated glass. A) Difference absorption spectrum of $(PSS/PDDA)_5$–$(GOx/PDDA)_7$ vs. $(PSS/PDDA)_5$ showing a peak around 670 nm. B) Integrated peak area between 640 nm and 710 nm as a function of GOx/PDDA layer number for $(PSS/PDDA)_5$–$(GOx/PDDA)_n$ with $1 \le n \le 8$.

3.2. Kinetic investigations using SECM

One of our aims is to prepare enzymatically active microstructures based on LbL films. In order to characterise the local kinetics of the embedded enzyme, we used SECM and tested the concept by investigating homogeneous films of GOx–PDDA multilayer by SECM approach curves in the feedback mode. For this purpose, the natural oxidant of the enzyme (O_2) was replaced by ferrocinium methanol (Fc^+) which was generated at the UME by oxidation of ferrocene methanol (Fc) provided in sub-millimolar concentration in the deaerated working solution. Although Ar or N_2 was continuously passed over the electrolyte during our measurements, a rigorous exclusion of O_2 is not possible in our setup. However, we were unable to measure an O_2 reduction current with the Pt electrode. Even if small traces remained in the cell, they were continuously consumed by the GOx-containing layer on the sample. If the UME approaches the sample, the O_2 diffusion to the sample regions underneath the UME is further blocked by the presence of the UME with its insulating shield, which further decreases a possible competition between the electron acceptors Fc^+ (high flux from UME) and O_2. The amount of Fc^+ consumed (and thus the amount of Fc regenerated) by the enzyme is detected as an additional source of Fc that leads to an enhanced oxidation current at the UME (Fig. 2). This response can be compared to a system without enzymatic reaction at the sample. Such a comparison is conveniently obtained by recording an approach curve in a glucose-free solution using Fc as mediator. In this case the enzymatic reaction cannot proceed and the UME current is determined exclusively by the hindered diffusion of the Fc from the solution bulk to the UME. The response has been theoretically obtained by digital simulations of varying accuracy [37]. The sample behaves like an inert sample (like glass) and such a measurement can serve as a control.

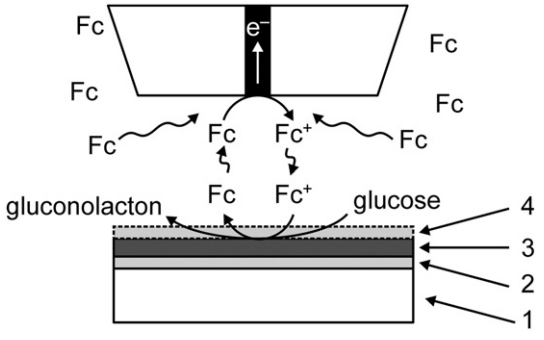

Fig. 2. Schematic setup of the SECM experiments. The sample consists of an aminated glass slide (1) which is covered by a precursor film $(PSS/PDDA)_5$ (2), the glucose oxidase (GOx)-containing PE multilayer $(GOx/PDDA)_n$ (3) and in some cases an inert PE multilayer film $(PSS/PDDA)_m$ (4). At the ultramicroelectrode (UME) ferrocene methanol (Fc) is oxidised to ferrocinium methanol (Fc^+) which acts as electron acceptor for GOx.

Usually the following (simplified) reaction mechanism is used to analyse the enzymatic reaction of glucose oxidase with glucose and a one-electron mediator [38,39]:

$$GOx_{ox} + \text{glucose} \underset{k_{-1}}{\overset{k_1}{\rightleftarrows}} [GOx_{ox}\cdot\cdot\cdot\text{glucose}] \quad (1)$$

$$[GOx_{ox}\cdot\cdot\cdot\text{glucose}] \xrightarrow{k_2} GOx_{red} + \text{gluconolactone} \quad (2)$$

$$GOx_{red} + 2Fc^+ \xrightarrow{k_3} GOx_{ox} + 2Fc \quad (3)$$

The reaction mechanism can be transferred to a rate law following earlier reports [25,38,39].

$$\frac{dc_{Fc^+}}{dt} = \frac{2k_2 \cdot \Gamma_{GOx}}{\frac{K_{M,glc}}{c_{glc}} + \frac{K_{M,Fc^+}}{c_{Fc^+}} + 1} \quad (4)$$

with

$$K_{M,glc} = \frac{k_{-1} + k_2}{k_1} \quad (5)$$

$$K_{M,Fc^+} = \frac{k_2}{k_3} \quad (6)$$

The expression can be simplified if the concentration of glucose c_{glc} is much bigger than the Michaelis–Menten constant

$K_{M,glc}$ for glucose. Apparent pseudo first order kinetics with respect to the SECM mediator can be observed if $c_{Fc^+} < K_{M,Fc^+}$.

SECM approach curves have been simulated for first order reactions at the sample surface [21]. From these data an analytical approximation has been derived [23] that can be used to extract kinetic data of the immobilised enzyme if it works in the first order regime with respect to Fc^+ [40].

$$I_T(L) = I_{T,ins}(L) + I_S(L)\left(1 - \frac{I_{T,ins}(L)}{I_{T,cond}(L)}\right) \quad (7)$$

$$I_S(L) = \frac{0.78377}{L\left(1+\frac{1}{\kappa L}\right)} + \frac{0.68 + 0.3315\exp\left(\frac{-1.0672}{L}\right)}{1 + \frac{(11/\kappa L)+7.3}{110-40L}} \quad (8)$$

$I_T = i_T(d)/i_{T,\infty}$ is the normalised current ($i_{T,\infty}$ — current at quasi infinite distance to the surface, i_T — UME current at a given working distance d), $L = d/r_T$ is the normalised distance (r_T — radius of the active area of the UME), $I_{T,ins}$ is the normalised UME current with no reaction at the sample (hindered diffusion) [41], and $I_{T,cond}$ is the normalised UME current under the condition of diffusion-controlled reaction rate at the sample surface [41].

$$I_{T,ins}(L) = \frac{1}{0.40472 + \frac{1.60185}{L} + 0.58819\exp\left(\frac{-2.37294}{L}\right)} \quad (9)$$

$$I_{T,cond}(L) = 0.72627 + \frac{0.76651}{L} + 0.26015\exp\left(\frac{-1.41332}{L}\right) \quad (10)$$

Fitting of experimental approach curves to Eqs. (7) and (8) yields a normalised reaction rate constant κ:

$$\kappa = \frac{k_{eff} r_T}{D} \quad (11)$$

where k_{eff} is the apparent first order reaction rate constant, and D is the diffusion coefficient of Fc. Details of the fitting procedures are given elsewhere [24,26]. Briefly, experimental data are normalised with respect to $i_{T,\infty}$ and r_T. Afterwards they are fitted to simulated working curves. Adjustable parameters are the normalised first order reaction rate constant κ, $i_{T,\infty}$, r_T, and the smallest distance d_0 between the active part of the probe and the substrate. r_T and d_0 are obtained independently from approach curves to GOx multilayer films without glucose present in the working solution and fitting to the theory for inert, insulating samples by adjusting r_T and d_0 [41]. Subsequently, the approach curve to the active enzyme layer is fitted by using fixed r_T and d_0 and adjusting κ and $i_{T,\infty}$.

3.3. Influence of glucose concentration

For the subsequent quantitative experiments, one enzyme substrate (glucose) must be provided in the regime of substrate saturation whereas the mediator (Fc/Fc^+) is reacting under pseudo first order conditions. A PDDA-terminated multilayer film containing three GOx–PDDA double layers [$(PSS/PDDA)_5$–$(GOx/PDDA)_3$] was investigated using glucose

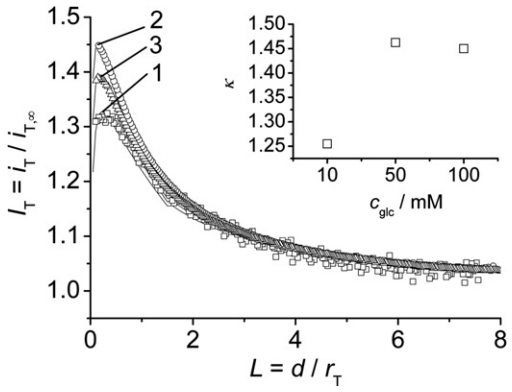

Fig. 3. SECM approach curves to $(PSS/PDDA)_5$–$(GOx/PDDA)_3$. Working solution contained 0.045 mmol L^{-1} Fc and different glucose concentrations: 10 mmol L^{-1} (1), 50 mmol L^{-1} (2), and 100 mmol L^{-1} (3); E_T=300 mV, v_T=0.87 μm s^{-1}. Symbols represent experimental data, solid lines correspond to theoretical data. Inset: κ values as a function of different glucose bulk concentrations.

bulk concentrations between 10 mmol L^{-1} and 100 mmol L^{-1} in order to verify experimentally that substrate saturation with respect to glucose is effective during recording of SECM approach curves. The approach curves were fitted to first order reaction kinetics and κ values were obtained (Fig. 3). The κ values with respect to Fc regeneration rate increase only slightly with c_{glc} that was varied over one order of magnitude. This reflects a slight increase of the overall conversion that can be expected if $c_{glc} > K_{M,glc}$ and the enzyme is almost saturated with respect to glucose at the lowest c_{glc} tested. Above 50 mmol L^{-1}, no further increase of κ values was observed (Fig. 3, inset) indicating complete saturation. Therefore, solutions containing 50 mmol L^{-1} glucose were used for all other experiments.

Saturation with respect to glucose at around 50 mmol L^{-1} is consistent with apparent Miachelis–Menten constants reported for immobilised GOx. Shu and Wilson immobilised GOx on a carbon paste electrode and found apparent $K_{M,glc}$ values in the range of (7.7–9.1) mmol L^{-1} [42]. Castner and Wingard Jr. used different techniques to immobilise GOx on a platinum electrode (silane-glutaraldehyde, allylamine-glutaraldehyde, albumin-glutaraldehyde) and reported apparent $K_{M,glc}$ values ranging from 12 to 36 mmol L^{-1} which was ascribed to different mass-transfer resistances [43]. Gregg and Heller immobilised GOx in poly(vinylpyridine) films and found an apparent $K_{M,glc}$ of 7.6 mmol L^{-1} [44]. Bourdillon et al. investigated GOx immobilised on glassy carbon electrode via antibody–antigen interaction and obtained $K_{M,glc}$ of 67 mmol L^{-1} [38]. In our experiments a regime of pseudo first order kinetics with respect to Fc^+ is even maintained if the glucose concentration is only slightly above $K_{M,glc}$ because the stoichiometry of the reaction in connection with the sub-millimolar concentration (0.045–0.9) mmol L^{-1} of the electron acceptor Fc^+ does not allow a significant deviation of the glucose concentration from the bulk value (50 mmol L^{-1}). Under these conditions the term $K_{M,glc}/c_{glc}$ in Eq. (4) is virtually constant and the reaction rate should depend only on c_{Fc^+}.

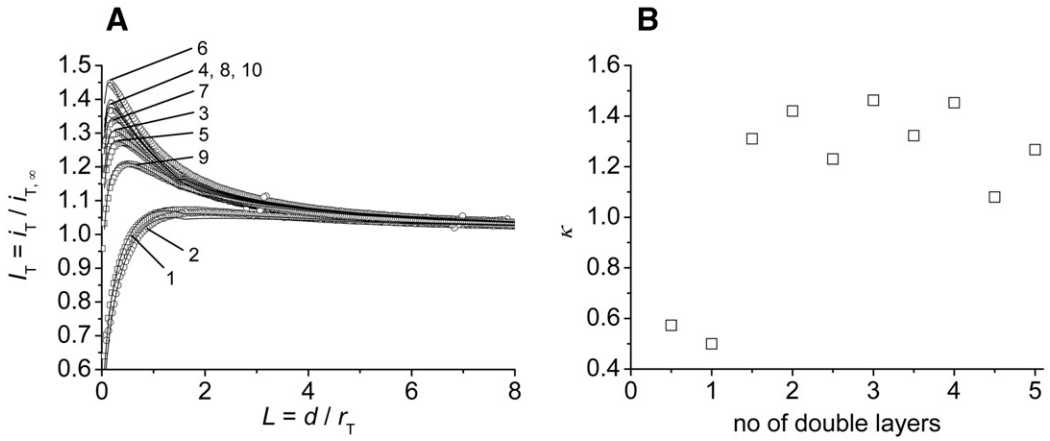

Fig. 4. SECM approach curves towards $(PSS/PDDA)_5$–$(GOx/PDDA)_n$ with $0.5 \le n \le 5$. Working solution contained 0.045 mmol L^{-1} Fc and 50 mmol L^{-1} glucose; E_T=300 mV, v_T=0.87 μm s^{-1}. A) Experimental (symbol) and theoretical (solid lines) approach curves for different number of GOx/PDDA double layers n: (1) 0.5, (2) 1, (3) 1.5, (4) 2, (5) 2.5, (6) 3, (7) 3.5, (8) 4, (9) 4.5, and (10) 5 (curves 4, 8 and 10 overlap). Integer n corresponds to PDDA-terminated films, non-integer n correspond to GOx-terminated films. B) κ values of PE multilayer films as function of layer number n.

3.4. Influence of layer number

Varying numbers of GOx multilayer films $(GOx/PDDA)_n$ with $0.5 \le n \le 5$ double layers were deposited on the precursor film $(PSS/PDDA)_5$ on an aminated glass slide. SECM approach curves were recorded (Fig. 4A) and analysed as described above leading to κ values (Fig. 4B). After two double layers κ values reach a plateau (Fig. 4B). Enzymatic conversion does not seem to increase further with increasing number of GOx layers. This indicates that only the topmost two layers contribute significantly to the overall conversion.

The low number of enzyme layers contributing to the overall conversion is seemingly contradictory to other publications dealing with similar systems [9,10,45,46]. A linear increase of enzymatic activity up to twelve bilayers has been reported [9]. In several studies, mass transport limitations *inside* the PE film resulted in a lower increase of the reaction rate per enzyme layer after a couple of bilayers [46]. The comparably low number of layers contributing significantly to the enzymatic conversion as measured by the UME may be attributed to mass transport limitations *inside* the PE film that may depend strongly on specific conditions under which the film was prepared such as adsorption conditions, counter ion nature and concentration, deposition mechanism (ionic interaction, specific biomolecular binding).

In addition to hindered mass transport inside the PE film two other possible limitations for the enzymatic conversion have to be considered. Firstly, glucose oxidase in lower layers might denaturate. It is generally accepted that the topmost layers of a PE multilayer film have different properties than the bulk film [47]. While the topmost layers still contain excess charges and have a lower mass density, deeper layers are electrostatically neutral and of constant mass density [47,48]. Our own scanning force microscopic (SFM) studies confirm that the film morphology changes significantly depending on the nature of the terminating layer (vide infra). This may also imply rearrangement of the GOx molecules if covered with further double layers.

Secondly, the concentration of the oxidant Fc^+ is very low. It would be possible that it is used up in the uppermost two layers and thus a contribution of the underlying layers would not occur. This can be tested by investigating the total flux of Fc formed by the GOx-containing PE multilayer as a function of Fc bulk concentration. The current equivalent $i_{T,FB}(L)$ of the Fc flux generated at the GOx-containing PE multilayer on the sample surface can be obtained from the UME current $i_T(L)$ at a certain normalised distance L. It is obtained by subtracting from experimental approach curves $i_T(L)$ the current contribution resulting from the hindered diffusion of Fc from the bulk solution to the UME, $i_{T,ins}(L)$ [40], which can be obtained from analytical approximations of digital simulations Eq. (9) [41]:

$$i_{T,FB}(L) = \left(I_T(L) - I_{T,ins}(L)\right) \cdot i_{T,\infty} \qquad (12)$$

$i_{T,FB}(L)$ has been evaluated for four different mediator bulk concentrations ranging from 0.045 mmol L^{-1} to 0.9 mmol L^{-1} (Fig. 5A, curves 1 to 4). The highest concentration is determined by the solubility of Fc in the used buffer.

An increase of $i_{T,FB}$ is observed for increasing mediator concentration c_{Fc}*. At distances $L>1$ the increase is linear confirming that the system operates in the regime of pseudo first order kinetics with respect to Fc^+ (Fig. 5A, inset curve 1). At L=0.26 the response for the highest c_{Fc}* falls below the value expected for a first order behaviour (Fig. 5A, inset curve 2). At such small working distances, the amount of UME-generated Fc^+ has to be converted by a small area of the GOx-containing PE film and the amount of enzyme that is reached by Fc^+ is not sufficient to sustain a first order regime. The concentration range in which a deviation from pseudo first order kinetics is observed is consistent with K_{M,Fc^+} values reported in literature [38]. In addition one must consider that c_{Fc^+} at the sample surface does not reach the bulk concentration of Fc since there is a steep concentration gradient between the UME and the sample surface. Therefore, it is clear that the enzyme is not saturated with respect to Fc^+. We noted that the approach curves recorded for c_{Fc}* >0.09 mmol L^{-1} could not be fitted to the theoretical

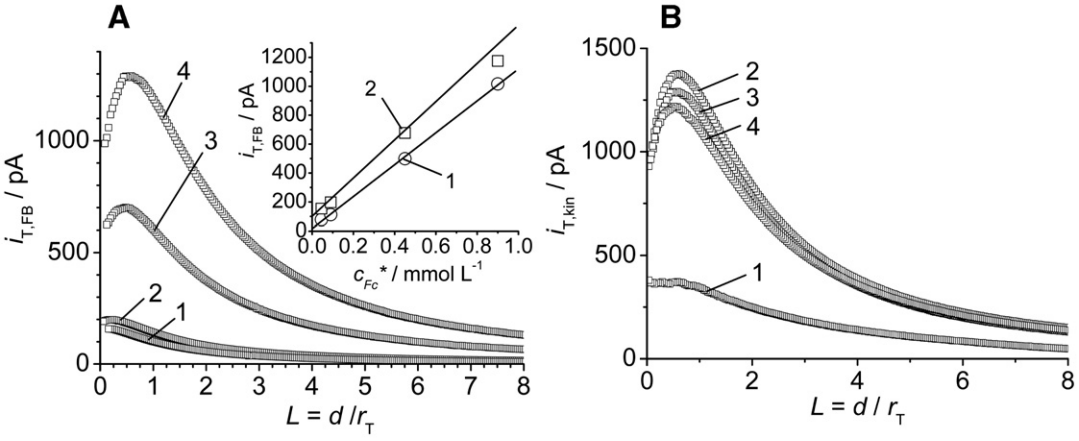

Fig. 5. SECM approach curves to $(PSS/PDDA)_5$–$(GOx/PDDA)_n$ multilayers using different Fc concentrations. A) Current equivalent $i_{T,FB}(L)$ generated at the $(PSS/PDDA)_5$–$(GOx/PDDA)_2$–GOx film ($i_{T,FB}(L)=[I_T(L)-i_{T,ins}(L)]\cdot i_{T,\infty}$). Working solution 50 mmol L^{-1} glucose and different concentrations of Fc: (1) 0.045 mmol L^{-1}, (2) 0.09 mmol L^{-1}, (3) 0.45 mmol L^{-1}, or (4) 0.9 mmol L^{-1}; E_T=300 mV, v_T=0.87 μm s^{-1}. Inset: Current equivalent $i_{T,FB}$ as a function of c_{Fc}^* at given normalised distances L: (1) 1.4, (2) 0.26. B) Current equivalent $i_{T,FB}(L)$ as a function of numbers of double layers n: (1) 0.5, (2) 1.5, (3) 2.5, and (4) 4.5. Working solution 0.9 mmol L^{-1} Fc and 50 mmol L^{-1} glucose; E_T=300 mV, v_T=0.87 μm s^{-1}.

curves according to Eqs. (7) and (8). Many repetitions with UME with RG=10 showed a systematic deviation from the theoretically predicted shape of the approach curve. If the current maximum was correctly adjusted to the model, it occurred at larger distances L than predicted by Eqs. (7) and (8). If the rising part of the experimental curve was adjusted to the model, the maximum current differed significantly from the prediction by Eqs. (7) and (8). The thickness of the film is about 20–100 nm and therefore insignificant to the positional uncertainty in L in the approach curves. Hence, partial penetration of the PE film cannot be the reason for this deviation. In agreement with the results shown in the inset of Fig. 5A, we interpret this observation as an indication for a deviation from the pseudo first order regime with respect to Fc^+.

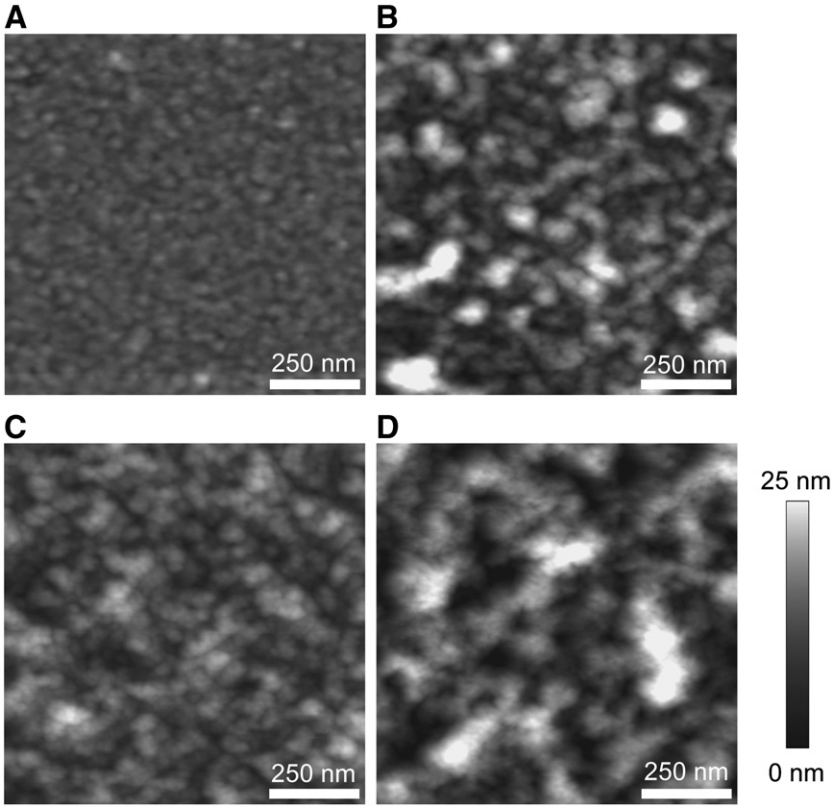

Fig. 6. SFM micrographs of differently terminated PE multilayer films. A) Precursor layer $(PSS/PDDA)_5$; B) GOx-terminated film $(PSS/PDDA)_5$–$(GOx/PDDA)_2$–GOx; C) PDDA-terminated film $(PSS/PDDA)_5$–$(GOx/PDDA)_3$; D) GOx-terminated film $(PSS/PDDA)_5$–$(GOx/PDDA)_3$–GOx. Inserted scale bars are 250 nm, z-range is 25 nm for all images.

At very small UME sample distances the flux imposed by the UME on the GOx-containing PE multilayer becomes so large that the film does not operate in the first order regime.

Recording $i_{T,FB}(L)$ for the highest mediator concentration $c_{Fc}^{*}=0.9$ mmol L^{-1} as a function of PE double layer number does not show a significant increase of $i_{T,FB}(L)$ for more than 2 double layers (Fig. 5B). This indicates that even at higher mediator concentrations deeply buried enzyme layers do not contribute to the flux of Fc^{+} measured by the UME.

The κ values in Fig. 4B indicate that the enzyme activity is higher for positively charged PDDA-terminated films. A reproducible odd–even pattern of κ is observed with respect to half layer numbers. Surprisingly, PDDA-terminated multilayers show higher κ values than GOx-terminated films if $n \geq 2$. Ferreyra et al. investigated a very similar system on glassy carbon electrodes by means of cyclic voltammetry at the support electrode and observed higher activity on negatively charged, GOx-terminated films [10]. Electrostatic effects were elaborated as a major reason by using different ferrocene derivatives. The source for the seemingly contradictory results is uncertain at the moment. Probably different mass transport pathways in the two experimental methods — SECM and cyclic voltammetry — influence the result. Assigning the effect to a certain process is difficult due to the large number of differently charged and neutral molecules involved that may undergo partitioning equilibria and various intermolecular interaction.

Interestingly, the odd–even pattern observed in the enzyme activity measurements (Fig. 4B) is also observed in SFM micrographs recorded for different layer numbers and film terminations (Fig. 6). While the precursor film is smooth (roughness mean square (RMS)=1.5 nm, Fig. 6A), the GOx-terminated film $(GOx/PDDA)_{2.5}$ comprises a significant roughness (RMS=5.0 nm, Fig. 6B). Features as big as 22 nm are observed (Fig. 7). They are much bigger than the size of a single GOx molecule (spherical diameter 8.2 nm [46]) indicating enzyme aggregation in Fig. 7. Aggregation of enzymes during LbL deposition has already been described frequently for GOx although less pronounced with PDDA as counter ion [6]. After adsorption of another layer of PDDA, the multilayer film is smoother and contains smaller grains than the GOx-terminated one (Fig. 6C, RMS=3.3). It can be speculated that GOx aggregates are broken up during adsorption of the next layer of PDDA and a more homogeneous distribution of the enzyme is achieved. Desorption of enzyme during the following PE adsorption has been described in literature [45]. This seems to be unlikely in this case as the enzyme activity increases after adsorbing the next layer of PDDA. The SFM image recorded after the next layer of GOx, $(GOx/PDDA)_{3.5}$ shows an increased roughness and larger aggregates (RMS=5.8 nm, Fig. 6D) that resemble that of the GOx-terminated layer of the previous coating cycle $(GOx/PDDA)_{2.5}$.

3.5. Covering layers

In order to estimate the mass transport limitation on the film activity, varying numbers of $(PDDA/PSS)_n$ layers with $0.5 \leq n \leq 6.5$ were deposited on $(GOx/PDDA)_{2.5}$ (three layers

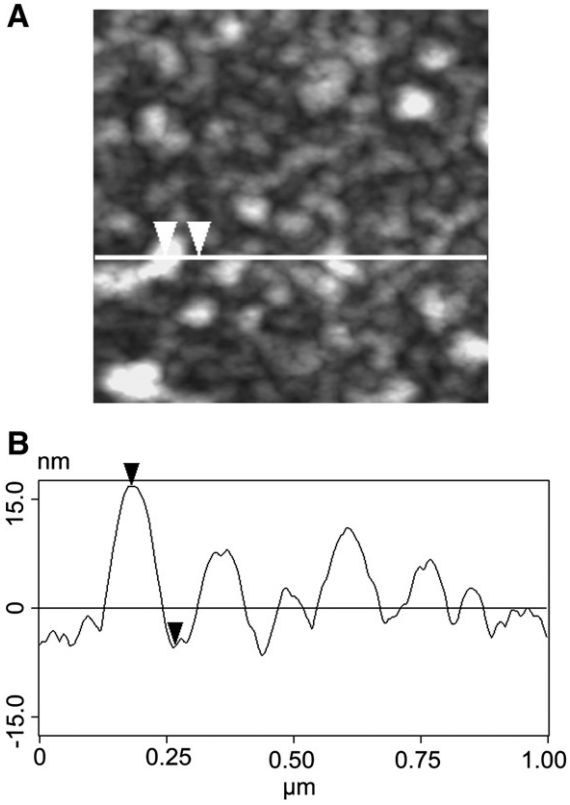

Fig. 7. Cross section extracted from an SFM micrograph of $(PSS/PDDA)_5$–$(GOx/PDDA)_2$–GOx. A) Grey-scale representation; image size is (1×1) μm^2. B) Cross section along line shown in part A). Vertical distance of arrows is 22.2 nm, horizontal distance is 85.9 nm.

of GOx). The enzymatic activity was investigated using the SECM. For half a covering double layer $(GOx/PDDA)_{2.5}$–PDDA an increase of reactivity is observed (Fig. 8B). This effect has already been discussed above. If the enzyme film is covered, however, with one double layer PDDA/PSS, the enzyme activity is already decreased to less than one half compared to the uncovered film (Fig. 8A and B). Further increase of the inert PDDA/PSS double layer number decreased further the enzymatic conversion in the system $(GOx/PDDA)_{2.5}$–$(PDDA/PSS)_n$ (Fig. 8B).

These results are in agreement with data published by Caruso and Schüler [45]. They covered multilayers of GOx and poly (allylamine hydrochloride) (PAH) multilayer films on polystyrene carrier particles with (PAH/PSS) multilayers. After deposition of five layers (PAH/PSS), enzyme activity had decreased to 50% compared to one covering layer. The stronger decrease of detected enzymatic activity might be due to more dense PE layers compared to the PAH/PSS system. Also, the comparably low mediator concentration in the SECM experiment might enhance the diffusional limitation inside the film as discussed above [9]. One also has to take into account that enzymes buried deeply in the film might denature because the polyelectrolyte interacts with charges of the protein and changes its conformation. A general comparison between different polyions with respect to denaturing a particular protein is problematic. However, a number of studies observed functional

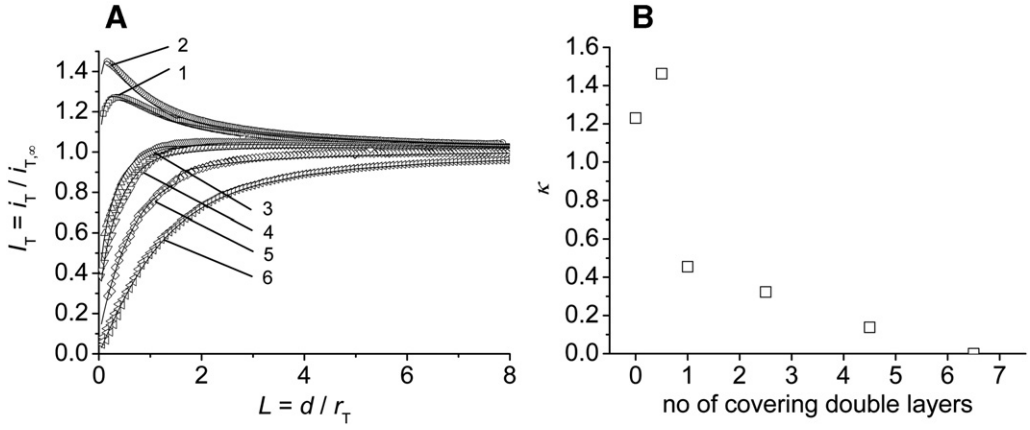

Fig. 8. SECM approach curves to $(PSS/PDDA)_5$–$(GOx/PDDA)_2$–GOx–$(PDDA/PSS)_n$ with $0 \le n \le 6.5$. Working solution 0.045 mmol L^{-1} Fc and 50 mmol L^{-1} glucose; E_T=300 mV, v_T=0.87 μm s^{-1}. A) Experimental (symbol) and theoretical (solid lines) approach curves for different number of PDDA/PSS double layers n: (1) 0, (2) 0.5, (3) 1, (4) 2.5, (5) 4.5, and (6) 6.5. B) κ values of the approach curves in part A.

proteins in multilayers. In the system investigated by Ferreyra et al. [10], $(GOx/PDDA)_n$ with $1 \le n \le 7$ on a modified glassy carbon electrode, a linear increase of enzymatic conversion with layer number was observed. This indicated that all enzyme layers contributed equally to the overall conversion and no denaturation took place in deeper layers. However in this system no polymeric polyanion was present.

3.6. Time dependence

In order to exclude a fast denaturation of GOx after the LbL deposition as a reason for the low number of enzyme layers contributing to the overall catalytic conversion, time-dependent activity measurements have been performed. A $(PSS/PDDA)_5$–$(GOx/PDDA)_5$ film on aminated glass slide was stored in buffer solution at room temperature and SECM approach curves were recorded repeatedly within 12 days after fabrication (Fig. 9). The κ values extracted from the approach curves decreased slowly with a half-life of approximately 5 days. However, a fast denaturation or decomposition of the enzyme layers during measurement (time scale of a few hours) could be excluded as a reason for the observed phenomena.

A comparison of the results of the SECM investigation of GOx-containing PE multilayers with previous studies, in which the enzymatic conversion was measured at the support electrode (biosensor configuration) shows one significant qualitative difference. In our system only the topmost GOx layers contribute significantly to the flux of Fc measured by the SECM probe outside the PE film. This observation is even more striking as other parameters of the film agree quite well with previous observations of similar films. The different findings may be at least partially a result of the different way the enzyme activity of the PE films was interrogated (Fig. 10). Unfortunately, the SECM investigation of enzymes on conducting supports (biosensor configuration) cannot provide quantitative results, because the Fc^+ can be regenerated by the enzymatic reaction but also by a heterogeneous electron transfer reaction at the conducting support. This configuration has been tested experimentally [49] and was discussed in depth elsewhere [20,50].

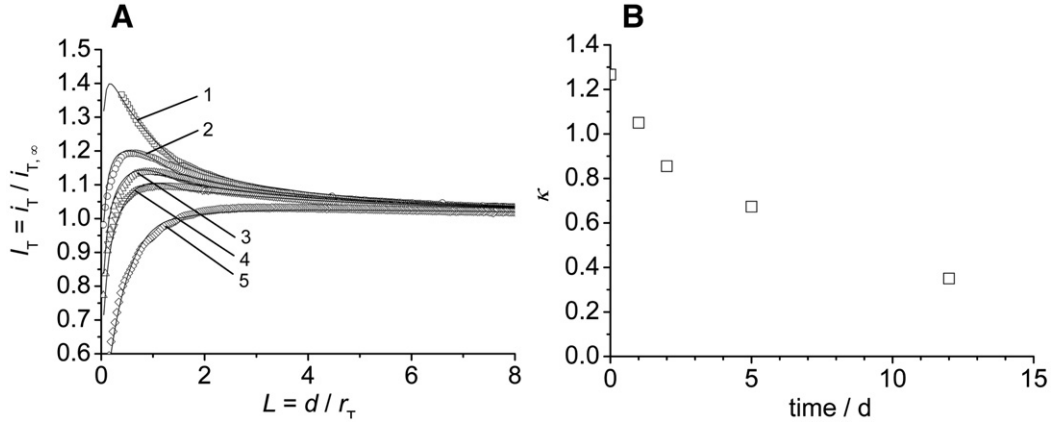

Fig. 9. A) SECM approach curves to $(PSS/PDDA)_5$–$(GOx/PDDA)_5$ after different storage time. Working solution 0.045 mmol L^{-1} Fc and 50 mmol L^{-1} glucose; E_T=300 mV, v_T=0.87 μm s^{-1}. Storage time in phosphate buffer at room temperature in days: (1) 0 (freshly prepared), (2) 1, (3) 2, (4) 5, and (5) 12. B) κ values extracted from approach curves in part A).

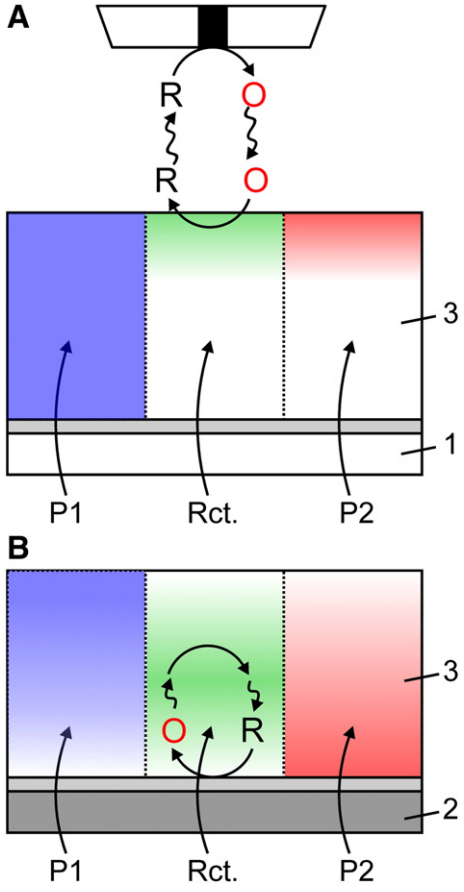

Fig. 10. Schematic comparison of the analysis of enzymatic conversion by electrochemical measurements at (A) SECM feedback experiments and (B) the support surface (biosensor configuration). O — oxidised form of the mediator, R — reduced form mediator form, (1) glass support with precursor layers, (2) support electrode with precursor layer, (3) GOx-containing PE multilayer film. The differently coloured section of the film visualise qualitatively the concentration gradient of glucose (blue, P1) and Fc^+ (red, P2). The reaction zone is shown in green (Rct.). The zones P1, P2 and Rct. in the schematics are displayed for clarity of the 2 overlapping concentration profiles inside the PE film and do *not* symbolise a lateral patterning in the experimental systems. The UME in part A is greatly reduced in size with respect to the PE film and shall only indicate the source of Fc^+. (For interpretation of the references to colour in this figure legend, the reader is referred to the web version of this article.)

In the SECM experiments the concentration of the electron acceptor (Fc^+) is much lower than that of the substrate glucose. This implies that the glucose concentration is essentially constant and high throughout the entire film so that mass transport limitations for glucose should not be important in the study. In contrast, Fc^+ mass transport inside the film is limiting and can be a reason why a significant conversion occurs only in the topmost layers even if the intrinsic activity of deeper GOx layer is maintained (Fig. 10A). The consumed glucose in the topmost layers is easily re-supplied by diffusion from the solution bulk. The requirement of Fc to diffuse across the UME sample distance in solution imposes an upper limit on the Fc^+ flux that can be obtained. It is given by Eq. (10). However, none of our experiments comes even close to that limit.

In the biosensor configuration glucose diffuses from the solution into the film while the electron acceptor diffuses from the supporting electrode into the film (Fig. 10B). Therefore, no upper limit of the mediator flux is imposed by a macroscopic diffusion in solution and mediator recycling can be very effective depending on details of the interfacial and PE film structure. Considering a switch-on experiment, glucose is first converted at the electrode–PE film interface and requires delivery of glucose across the PE multilayer film. If this cannot be sustained, the electron acceptor will also reach further GOx layers before being completely consumed. In the steady-state a mixed control regime will be established that may depend on the mass transport of the electron acceptor, or glucose inside the film, and depending on the experimental conditions, of glucose in the solution. In this consideration GOx-containing LbL films tend to give higher apparent $K_{M,glc}$ values [51] than other immobilisation techniques [42,44]. Anicet et al. [9] also reported increased diffusion limitations at low mediator concentrations using cyclic voltammetry at the support electrode.

In addition, structural aspects of the PE films must be kept in mind because PE films are not homogeneous across the entire film thickness. The outer layers have a lower mass density than the inner layers [47,48]. In SECM experiments diffusion of Fc^+ occurs from the solution side into the loosely packed topmost layers. Therefore enzyme accessibility is much higher than that of enzymes in deeper layers. In agreement with this notion, most of the conversion occurs in the first two double layers in SECM experiments. In the biosensor configuration, the electron acceptor enters from the supporting electrode into already densely packed layers, where accessibility of active enzyme centres is generally lower and does not differ so much in the lowest and in further layers. Therefore the electron acceptor may reach further layers which also contribute to the total conversion. Furthermore, details of the deposition procedure, such as use of additional interaction to stabilise the films may change mass transport conditions inside the film that depends on a delicate interplay of many factors.

4. Conclusion

In this study, SECM approach curves have been used to analyse enzymatic activity of GOx/PDDA multilayer films. It has been found that only the topmost two layers contribute significantly to the overall reaction. Probably, mass transport limitations inside the film and consumption of Fc^+ in the topmost layers are the reasons for this behaviour. This agrees with the finding that covering layers of inert polyelectrolytes (PDDA/PSS) strongly suppress enzymatic conversion.

Depending on the film termination, an odd–even pattern of the enzymatic activity has been found. It correlates with a periodically changing surface morphology of the films.

References

[1] G. Decher, J.D. Hong, Buildup of ultrathin multilayer films by a self-assembly process: II. Consecutive adsorption of anionic and cationic bipolar amphiphiles and polyelectrolytes on charged surfaces, Ber. Bunsen-Ges. 95 (1991) 1430–1434.

[2] G. Decher, Fuzzy nanoassemblies: toward layered polymeric multicomposites, Science 277 (1997) 1232–1237.
[3] Y. Lvov, K. Ariga, T. Kunitake, Layer-by-layer assembly of alternate protein/polyion ultrathin films, Chem. Lett. (1994) 2323–2326.
[4] M. Campas, C. O'Sullivan, Layer-by-layer biomolecular assemblies for enzyme sensors, immunosensing, and nanoarchitectures, Anal. Lett. 36 (2003) 2551–2569.
[5] I. Ichinose, K. Kuroiwa, Y. Lvov, T. Kunitake, Recent progress in the surface sol–gel process and protein multilayers, in: G. Decher, J.B. Schlenoff (Eds.), Multilayer Thin Films, Wiley-VCH, Weinheim, 2003, pp. 155–175.
[6] Y. Lvov, K. Ariga, I. Ichinose, T. Kunitake, Assembly of multicomponent protein films by means electrostatic layer-by-layer adsorption, J. Am. Chem. Soc. 117 (1995) 6117–6123.
[7] M. Onda, Y. Lvov, K. Ariga, T. Kunitake, Sequential actions of glucose oxidase and peroxidase in molecular films assembled by layer-by-layer alternate adsorption, Biotechnol. Bioeng. 51 (1996) 163–167.
[8] D.S. Patel, R.K. Aithal, G. Krishna, Y.M. Lvov, M. Tien, D. Kuila, Nanoassembly of manganese peroxidase and lignin peroxidase from *P. chrysosporium* for biocatalysis in aqueous and non-aqueous media, Colloids Surf., B Biointerfaces 43 (2005) 13–19.
[9] N. Anicet, C. Bourdillon, J. Moiroux, J.-M. Saveant, Electron transfer in organized assemblies of biomolecules. Step-by-step avidin/biotin construction and dynamic characteristics of a spatially ordered multilayer enzyme electrode, J. Phys. Chem., B 102 (1998) 9844–9849.
[10] N. Ferreyra, L. Coche-Guerente, P. Labbe, Construction of layer-by-layer self-assemblies of glucose oxidase and cationic polyelectrolyte onto glassy carbon electrodes and electrochemical study of the redox-mediated enzymatic activity, Electrochim. Acta 49 (2004) 477–484.
[11] S. Zhang, W. Yang, Y. Niu, C. Sun, Multilayered construction of glucose oxidase and poly(allylamine)ferrocene on gold electrodes by means of layer-by-layer covalent attachment, Sens. Actuators, B 101 (2004) 387–393.
[12] V. Rosca, I. Catalin Popescu, Kinetic analysis of horseradish peroxidase "wiring" in redox polyelectrolyte-peroxidase multilayer assemblies, Electrochem. Commun. 4 (2002) 904–911.
[13] M.K. Ram, P. Bertoncello, H. Ding, S. Paddeu, C. Nicolini, Cholesterol biosensors prepared by layer-by-layer technique, Biosens. Bioelectron. 16 (2001) 849–856.
[14] Y. Sun, X. Zhang, C. Sun, J. Shen, Fabrication of ultrathin film containing bienzyme of glucose oxidase and glucoamylase based on electrostatic interaction and its potential application as a maltose sensor, Macromol. Chem. Phys. 197 (1996) 147–153.
[15] G. Liu, Y. Lin, Amperometric glucose biosensor based on self-assembling glucose oxidase on carbon nanotubes, Electrochem. Commun. 8 (2006) 251–256.
[16] K. Habermüller, M. Mosbach, W. Schuhmann, Electron-transfer mechanism in amperometric biosensors, Fresenius' J. Anal. Chem. 366 (2000) 560–568.
[17] P.T. Hammond, Chemistry directed deposition via electrostatic and secondary interactions: a nonlithographic approach to patterned polyelectrolyte multilayer systems, in: G. Decher, J.B. Schlenoff (Eds.), Multilayer Thin Films, Wiley-VCH, Weinheim, 2003, pp. 271–299.
[18] A.J. Bard, M.V. Mirkin (Eds.), Scanning Electrochemical Microscopy, Marcel Dekker, Inc., New York, 2001, Basel.
[19] P. Sun, F.O. Laforge, M.V. Mirkin, Scanning electrochemical microscopy in the 21st century, Phys. Chem. Chem. Phys. 9 (2007) 802–823.
[20] G. Wittstock, M. Burchardt, S.E. Pust, Y. Shen, C. Zhao, Scanning electrochemical microscopy for direct imaging of reaction rates, Angew. Chem., Int. Ed. Engl. 46 (2007) 1584–1617.
[21] A.J. Bard, M.V. Mirkin, P.R. Unwin, D.O. Wipf, Scanning electrochemical microscopy. 12. Theory and experiment of the feedback mode with finite heterogeneous electron-transfer kinetics and arbitrary substrate size, J. Phys. Chem. 96 (1992) 1861–1868.
[22] D.O. Wipf, A.J. Bard, Scanning electrochemical microscopy: VII effect of electron transfer rate at the substrate on the tip feedback current, J. Electrochem. Soc. 138 (1991) 469–474.
[23] C. Wei, A.J. Bard, M.V. Mirkin, Scanning electrochemical microscopy. 31. Application of SECM to the study of charge transfer processes at the liquid/liquid interface, J. Phys. Chem. 99 (1995) 16033–16042.
[24] S.E. Pust, D. Scharnweber, S. Baunack, G. Wittstock, Electron transfer kinetics at oxide films on metallic biomaterials: scanning electrochemical microscopy studies of Ti6Al4V, J. Electrochem. Soc. 154 (2007) C508–C514.
[25] D.T. Pierce, P.R. Unwin, A.J. Bard, Scanning electrochemical microscopy. 17. Studies of enzyme-mediator kinetics for membrane- and surface-immobilized glucose oxidase, Anal. Chem. 64 (1992) 1795–1804.
[26] G. Wittstock, M. Burchardt, C. Nunes Kirchner, Scanning electrochemical microscopy in biosensor research, in: S. Alegret, A. Merkoçoi (Eds.), Electrochemical Sensor Analysis, Elsevier, Amsterdam, 2007, pp. 907–939.
[27] C.A. Wijayawardhana, G. Wittstock, H.B. Halsall, W.R. Heineman, Spatially addressed deposition and imaging of biochemically active bead microstructures by scanning electrochemical microscopy, Anal. Chem. 72 (2000) 333–338.
[28] T. Wilhelm, G. Wittstock, Generation of periodic enzyme patterns by soft lithography and activity imaging by scanning electrochemical microscopy, Langmuir 18 (2002) 9485–9493.
[29] H. Shiku, T. Takeda, H. Yamada, T. Matsue, I. Uchida, Microfabrication and characterization of diaphorase-patterned surface by scanning electrochemical microscopy, Anal. Chem. 67 (1995) 312–317.
[30] H. Shiku, I. Uchida, T. Matsue, Microfabrication of alkylsilanized glass substrate by electrogenerated hydroxyl radical using scanning electrochemical microscopy, Langmuir 13 (1997) 7239–7244.
[31] M. Maciejewska, D. Schaefer, W. Schuhmann, SECM imaging of spatial variability in biosensor architectures, Electrochem. Commun. 8 (2006) 1119–1124.
[32] J.H. Pazur, Glucose oxidase from *Aspergillus niger*, Methods Enzymol. 9 (1966) 82–87.
[33] C.A. Nijhuis, J.K. Sinha, G. Wittstock, J. Huskens, B.J. Ravoo, D.N. Reinhoudt, Controlling the supramolecular assembly of redox-active dendrimers at molecular printboards by scanning electrochemical microscopy, Langmuir 22 (2006) 9770–9775.
[34] T. Wilhelm, G. Wittstock, Localised electrochemical desorption of gold alkanethiolate monolayers by means of scanning electrochemical microscopy (SECM), Microchim. Acta 133 (2000) 1–9.
[35] C. Nunes Kirchner, S. Szunerits, G. Wittstock, Scanning electrochemical microscopy (SECM) based detection of oligonucleotide hybridization and simultaneous determination of the surface concentration of immobilized oligonucleotides on gold, Electroanalysis 19 (2007) 1258–1267.
[36] C. Kranz, M. Ludwig, H.E. Gaub, W. Schuhmann, Lateral deposition of polypyrrole lines by means of the scanning electrochemical microscope, Adv. Mater. 7 (1995) 38–40.
[37] R. Cornut, C. Lefrou, New analytical approximations for negative feedback currents with a microdisk SECM tip, J. Electroanal. Chem. 604 (2007) 91–100.
[38] C. Bourdillon, C. Demaille, J. Moiroux, J.M. Saveant, New insights into the enzymic catalysis of the oxidation of glucose by native and recombinant glucose oxidase mediated by electrochemically generated one-electron redox cosubstrates, J. Am. Chem. Soc. 115 (1993) 2–10.
[39] C. Bourdillon, C. Demaille, J. Gueris, J. Moiroux, J.M. Saveant, A fully active monolayer enzyme electrode derivatized by antigen–antibody attachment, J. Am. Chem. Soc. 115 (1993) 12264–12269.
[40] C. Zhao, G. Wittstock, Scanning electrochemical microscopy of quinoprotein glucose dehydrogenase, Anal. Chem. 76 (2004) 3145–3154.
[41] J.L. Amphlett, G. Denuault, Scanning electrochemical microscopy (SECM): an investigation of the effects of tip geometry on amperometric tip response, J. Phys. Chem., B 102 (1998) 9946–9951.
[42] F.R. Shu, G.S. Wilson, Rotating ring-disk enzyme electrode for surface catalysis studies, Anal. Chem. 48 (1976) 1679–1686.
[43] J.F. Castner, L.B. Wingard Jr., Mass transport and reaction kinetic parameters determined electrochemically for immobilized glucose oxidase, Biochemistry 23 (1984) 2203–2210.
[44] B.A. Gregg, A. Heller, Cross-linked redox gels containing glucose oxidase for amperometric biosensor applications, Anal. Chem. 62 (1990) 258–263.
[45] F. Caruso, C. Schuler, Enzyme multilayers on colloid particles: assembly, stability, and enzymatic activity, Langmuir 16 (2000) 9595–9603.

[46] M. Onda, K. Ariga, T. Kunitake, Activity and stability of glucose oxidase in molecular films assembled alternately with polyions, J. Biosci. Bioeng. 87 (1999) 69–75.
[47] G. Ladam, P. Schaad, J.C. Voegel, P. Schaaf, G. Decher, F. Cuisinier, In situ determination of the structural properties of initially deposited polyelectrolyte multilayers, Langmuir 16 (2000) 1249–1255.
[48] J.B. Schlenoff, S.T. Dubas, Mechanism of polyelectrolyte multilayer growth: charge overcompensation and distribution, Macromolecules 34 (2001) 592–598.
[49] C. Kranz, G. Wittstock, H. Wohlschläger, W. Schuhmann, Imaging of microstructured biochemically active surfaces by means of scanning electrochemical microscopy, Electrochim. Acta 42 (1997) 3105–3111.
[50] G. Wittstock, W. Schuhmann, Formation and imaging of microscopic enzymatically active spots on an alkanethiolate-covered gold electrode by scanning electrochemical microscopy, Anal. Chem. 69 (1997) 5059–5066.
[51] S. Zhang, W. Yang, Y. Niu, C. Sun, Multilayered construction of glucose oxidase on gold electrodes based on layer-by-layer covalent attachment, Anal. Chim. Acta 523 (2004) 209–217.